Published in final edited form as:
Nano Life. 2010 ; 1(01n02): . doi:10.1142/S1793984410000067.

MAGNETIC NANOPARTICLE HYPERTHERMIA IN CANCER TREATMENT

Andrew J. Giustini,
Dartmouth Medical School and the Thayer School of Engineering, Dartmouth College, Hanover, New Hampshire 03755, USA, andrew.j.giustini@dartmouth.edu

Alicia A. Petryk[*],
Thayer School of Engineering, Dartmouth College, Hanover, New Hampshire 03755, USA

Shiraz M. Cassim[†],
Thayer School of Engineering, Dartmouth College, Hanover, New Hampshire 03755, USA

Jennifer A. Tate[‡],
Thayer School of Engineering, Dartmouth College, Hanover, New Hampshire 03755, USA

Ian Baker[§], and
Thayer School of Engineering, Dartmouth College, Hanover, New Hampshire 03755, USA

P. Jack Hoopes
Dartmouth Medical School and the Thayer School of Engineering, Dartmouth College, Hanover, New Hampshire 03755, USA

Abstract

The activation of magnetic nanoparticles (mNPs) by an alternating magnetic field (AMF) is currently being explored as technique for targeted therapeutic heating of tumors. Various types of superparamagnetic and ferromagnetic particles, with different coatings and targeting agents, allow for tumor site and type specificity. Magnetic nanoparticle hyperthermia is also being studied as an adjuvant to conventional chemotherapy and radiation therapy. This review provides an introduction to some of the relevant biology and materials science involved in the technical development and current and future use of mNP hyperthermia as clinical cancer therapy.

Keywords

Magnetic nanoparticle; hyperthermia; cancer; tumor

1. Background

After decades of intense study and numerous clinical trials, most forms of human cancer are still not curable. The reasons for this are multifactorial. “Cancer” has multiple etiologies and manifestations. Each of these is distinct and responds differently to therapies. The primary limiting factors are the lack of understanding of the mechanisms of tumor development and

[*]alicia.a.petryk@dartmouth.edu
[†]shiraz.m.cassim@dartmouth.edu
[‡]jennifer.a.tate@dartmouth.edu
[§]ian.baker@dartmouth.edu

of therapeutic intervention. While there have been some successes in treating certain types of neoplasms,[1,2] many tumor types are refractory to modern therapies.[3]

Over the past several decades, the principle types of cancer therapies have been chemotherapy, radiation therapy and surgery. Additional modalities, such as therapeutic hyperthermia, have achieved some success but are not yet considered standard-of-care therapies.

The primary reasons for hyperthermia's inability to enter mainstream cancer therapy have been: lack of differential normal tissue:cancer cytotoxicity, inability to target hyperthermia directly to tumors and an insufficient understanding of the mechanism of hyperthermia cytotoxicity.[4] In 1991, Roizin-Towle and Pirro studied the sensitivity of various cell types to hyperthermia. The authors compared the survival of normal and neoplastic human and rodent cell types, *in vitro*, as they were exposed to different thermal doses. The authors showed that, while all cell types could be killed by specific thermal doses, tumor cells did not display increased sensitivity to the treatment compared to normal cells.[4] This lack of inherent difference in normal versus tumor tissue sensitivity (therapeutic ratio) is unlike the differential responses of normal and cancerous tissue to radiation and chemotherapy. Their work showed that in order for hyperthermia to succeed as a cancer therapy, its mode of delivery must compensate for the lack of differential toxicity by localizing heat specifically to tumor cells. The implication of this finding was that, for hyperthermia to be therapeutically effective, it would have to be localized specifically to tumor tissue. Although cancerous tissues may be more sensitive to heat damage *in vivo* due to an insufficient blood supply, clinically available technologies (RF, microwave, ultrasound, conductive) have not been able to target heat specifically to tumors — especially metastatic tumors — in a clinically effect manner.

Recently, hyperthermia directed specifically to cancer cells through the use of magnetic nanoparticles heated with alternating magnetic fields has been used as a novel cancer therapy. This paper will explore this new application of magnetically-induced hyperthermia in cancer therapy.

2. Therapeutic Index (TI)

The challenge of cancer therapy is to control the tumor without unacceptable normal tissue toxicity. The terms "therapeutic index" (TI) or "therapeutic ratio" are used to quantify the ratio of a therapy's treatment potential in relation to its normal tissue toxicities. This measure can be used for populations of people or of cells to examine the relative effectiveness of a therapy. Therapies with high therapeutic index are essential for clinical success and can be achieved by exploiting differences in diseased tissue and normal tissue.

The similarity between normal and neoplastic tissue makes it difficult to develop therapies which will specifically kill tumor cells. This limitation explains many of the side effects seen with traditional antineoplastic chemotherapeutics. Unfortunately, many first line-chemotherapeutics do not have enough inherent selectivity. For example, Cisplatin — the most commonly used anti-neoplastic agent in the United States — can cause significant toxicity in bone marrow, gastrointestinal, and peripheral nerve cells.[5]

Currently there are three major types of antineoplastic therapy: (1) Surgical oncology relies on imaging techniques to delineate tumor tissue from normal tissue and then relies on the judgment of the surgeon and pathologist to determine which tissue to actually remove. Surgical oncology can be successful at controlling local neoplastic disease; it is, however, often challenged in the metastatic environment. (2) Use of chemotherapy has largely relied on exploitation of rapid cell division to kill cells, since most neoplasms divide rapidly.[6]

Chemotherapy is also able to address tumor cells at virtually any site in the body. As noted previously, this approach can lead to severe toxicities in normal tissue and often with insufficient TI. (3) Radiation therapy has maximized TI by exploiting the suboptimal DNA damage repair mechanisms in tumor tissue, which causes neoplastic tissue to be more radiation-sensitive than normal tissue. None of these therapies, alone or in concert, has led to reliably curative therapy for most neoplasms. Combining different types of therapies, however, can improve the therapeutic index of the treatments by having nonadditive normal tissue side effects but additive or synergistic therapeutic effects.[7,8]

3. Magnetic Nanoparticle Hyperthermia (mNPH)

In 1957, Gilchrist *et al*. demonstrated that lymph nodes could be inductively heated to kill lymphatic metastases after the administration of magnetic particles.[9] In these experiments, 5 mg of 20–100 nm diameter Fe_2O_3 particles were delivered to lymph nodes (47 mg of Fe_2O_3 per gram of tissue). A temperature rise of 14°C was seen following an exposure to an alternating magnetic field (AMF) of 200–240 Oe (16–19.2 kA/m) at 1.2 MHz.[9] Because no control experiments were reported, there remains the distinct possibility that, because of the high frequency used, much of the temperature rise was produced directly by the induced electric field rather than through nanoparticle heating. Subsequently, various methods of heat delivery were tested as cancer treatment modalities.[10,11] Generally, these techniques achieved limited success.

In the mid-1990s, the idea of using nanoparticle hyperthermia to treat tumors was revisited.[12] This method involved the injection of magnetic nanoparticles directly into tumors and exciting these nanoparticles with alternating magnetic fields (AMFs) to produce heat. Further progress has been made in directing nanoparticles to tumors with targeting agents such as antibodies.[13–16] Nanoparticle hyperthermia appears well-suited as an effective tumor therapy if (1) the concentration of particles in the tumor is both sufficiently high and significantly higher than in surrounding, normal tissue, and (2) the particles possess a high enough specific absorption rate (SAR, in Watts per gram)

$$\mathrm{SAR}=\frac{c\Delta T}{\Delta t}, \quad (1)$$

where c is the specific heat capacity, and ΔT is the temperature rise during the time interval (Δt) to deliver significant intratumoral doses of heat with AMFs that are well-tolerated by the normal tissues.

Currently, three different nanoparticle heating technologies for therapeutic purposes are being explored: (1) optical heating using lasers;[17] (2) ultrasound heating of small bubbles;[18] and (3) iron oxide heating due to AMF, using one of a variety of physical mechanisms generally termed hysteresis heating.[14,16,19–20] Each method has certain strengths and limitations. Optical methods heat particles effectively, but are severely limited by the attenuation of the laser light by tissue. Ultrasound heating may ultimately be promising, as the energy is focused to a selected location; it, however, suffers from speed of sound variation in most tissues and, in many applications, from the limited aperture of the applicator. Magnetic particle heating can be accomplished at depths necessary for treatment of tumors located virtually anywhere in the human body. The same particles used for heating may also be sufficient for medical imaging uses.

4. Hyperthermia as an Adjuvant to Radiation and Chemotherapy

It is well-known that exposing tumor cells to even mildly elevated temperatures sensitizes them to chemotherapy and radiation and may decrease their viability.[22,23] Although the

combination of hyperthermia with chemotherapeutics and radiation has shown great promise, to date the clinical impact has been modest.

One of the most successful uses of hyperthermia as an anti-neoplastic agent is as a treatment for intraperitoneal metastases from ovarian tumors. In this technology hyperthermia is used as a way of increasing the efficacy of certain chemotherapeutics.[11,24] While the nonfocused nature of this heating is beneficial in this case, the inability to deliver a uniform, sufficient thermal dose to all metastases has limited its clinical efficacy.

The lack of selective deposition of chemotherapeutic agents to cancer cells has limited the TI of traditional chemotherapeutics. Therefore, to date, chemotherapy for solid tumors has been used most effectively as an adjuvant to radiotherapy and/or surgery.[25] The ability to localize hyperthermia (magnetic nanoparticle hyperthermia, mNP) to cancer cells may greatly enhance the use of chemotherapy by reducing the necessary dose, thereby sparing normal tissue toxicity.[26]

A significant amount of effort has been dedicated to directing chemotherapeutics and controlling their release at the tumor site. Nanoparticle (both iron oxide-based and others) constructs which act as chemotherapeutic "carriers" are under development for both sustained and stimuli-activated release (by pH, electric fields, ultrasound, UV-light, radiation, and temperature).[27,28] These technologies have not yet been extensively tested *in vivo*.

Optimizing the pairing of chemotherapy and hyperthermia is dependent on tumor type, dose, clinical site and temperature. Studies have suggested that alkylating agents such as cyclophosphamide, ifosfamide and melphalan, may be most effective at 41.5°C,[29] while other therapeutics such as cisplatinum appear to be also effective at lower temperatures. The temporal optimization of hyperthermia-chemotherapeutic administration has yet to be achieved. Temperatures as low as 2–3°C above basal temperature have been shown to increase blood flow during, and for some time after, removal of the heat source from tumors. Studies suggest that this localized increase in blood flow assists in depositing chemotherapy within the heated tissue.[30,31]

The enhancement of radiotherapy with hyperthermia is well-documented.[32] The proposed mechanism for hyperthermia enhancement of therapeutic radiation is two-fold: (1) Ionizing radiation damages DNA and hyperthermia damages the proteins responsible for DNA repair.[33] (2) Hyperthermia is also able to kill cells in hypoxic regions of tumors which are more radio-resistant than cells in well-oxygenated areas.[23] The interaction of radiation and hyperthermia is influenced by a number of factors including temperature, duration of hyperthermia and the temporal relationship between hyperthermia and radiation. Optimization of the combination of hyperthermia and ionizing radiation has not yet been achieved due to these complex relationships[23]. MNP-based hyperthermia in combination with radio-therapy has shown early promise.[34] The combined use of magnetic nanoparticle-delivered radionucleotides in combination with nanoparticle hyperthermia is potentially attractive.[35]

5. Biological Heat Dose Equation

Cumulative Equivalent Minutes (CEMs) is a technique for determining and normalizing the total thermal dose (thermal history) of a heated tissue. The equation is:

$$\mathrm{CEM43°C}=tR^{(43-T)}, \quad (2)$$

where CEM43°C is the heat dose normalized to number of minutes at 43°C, t is the time at a given temperature in minutes, T is the average temperature during t, the time interval. R represents how many minutes would be required to account for a 1°C change in temperature above or below 43°C.[36] For human (rodent) cells, a typical value of R above the breakpoint is 0.45 (0.43) and value of R below the breakpoint is 0.25 (0.23).[36]

Thus, a population of rodent cells subjected to a temperature of 45°C for one minute would result in cytotoxicity equal to that of cells treated at 43°C for 5 min (CEM43°C = 5). A CEM43°C of 60 min yields approximately 50% cytotoxicity in CHO-10 B cells.[36]

6. Magnetic Nanoparticle Heating Mechanisms

Given the overall goal of producing localized hyperthermia in a tumor, the primary objective of nanoparticle design is to maximize the power deposition. This will enable the nanoparticles to be heated using an AMF to result in direct cytotoxicity, or to sensitize the tumor to radiation treatment or chemotherapy. Magnetic nanoparticles have also been used as MRI contrast agents.[37] The nanoparticles that are most easily imaged *in vivo*, however, are not necessarily the same as the ones that provide the greatest heating effect. It is also possible that mNP with the highest SAR values may have biocompatibility limitations.

The SAR is the parameter of magnetic nanoparticles that must be maximized to optimize the heating. Heating of a material in an AMF can occur by four mechanisms: (1) dielectric losses in a material of low electrical conductivity; (2) eddy currents losses in a material of high electrical conductivity; (3) frictional heating due to the physical rotation of an anisotropic magnetic particle and; (4) hysteresis losses in a magnetic material.

Dielectric and eddy current losses may lead to unacceptable normal tissue heating. Below, we discuss the use of the three other types of heating for nanoparticles. The heating effect in each case depends on the size, shape and coercivity of the particles, and the frequency and magnitude of the applied AMF.

6.1. Eddy current heating

Ivkov *et al*. examined the effects of induction from the application of an alternating pulsed magnetic field, at 153 kHz, on nude mice. They found that for field strengths below 700 Oe (20 min exposure), no adverse effects were observed. Field strengths greater than 950 Oe resulted in significant morbidity.[38] They also found that fields up to 1300 Oe could be applied with no observable adverse effects on the mice as long as the off/on time of the applied field was adjusted to limit the tissue heating.

The power density for eddy current heating is given by:

$$\mathrm{PE} = E f^2 H_{\max} d^2, \quad (3)$$

where E is the eddy current coefficient, f is the frequency, $H_{\max}$ is the maximum flux density, and d is the particle size.[9] The complication of eddy current heating of human tissue was first identified by Gilchrist *et al*. during their lymph node nanoparticle experiment.[9] Since PE increases as d^2, the eddy current heating becomes negligible on the nanoscale. While PE also increases as f^2, increasing the frequency beyond a few hundred kHz is not an attractive option, because it leads to the previously mentioned eddy current tissue heating.

6.2. Frictional heating

In a low-viscosity liquid, a magnetically anisotropic particle will physically rotate in an AMF. This effect has been used to mechanically damage cells.[39] The induced rotation leads

to frictional heating of the surrounding medium, and as a result, energy losses, which are referred to as Brownian losses. A good theoretical understanding of the associated frictional forces does not yet exist. A first-order empirical approximation is that the force is proportional to the velocity squared. Therefore, the energy would be given by the dot product between this force and the displacement of the particle. The power would be given by this energy divided by the frequency of the magnetic field. However, this approximation does not account for collective effects, or how the size and shape of the particle, as well as the viscosity of the liquid in which the nanoparticles are dispersed, affect the power dissipation. It is important to note that if the particle is immobilized, for example by being bound to a cell, this type of heating is unlikely to occur.[40,41]

6.3. Hysteresis heating

The fact that disparate categories of magnetic materials behave differently in magnetic fields is integral to understanding why some magnetic nanoparticles heat better than others. The relevant categories of materials in this case are paramagnetic, superparamagnetic and ferromagnetic. The simplest way of describing the responses of these materials to different magnetic fields is by plotting their magnetizations against applied magnetic fields (Fig. 1).

As can be seen in Fig. 1, the magnetizations (M) of paramagnetic and superparamagnetic materials have no remnant magnetization when there is no applied magnetic field. When either of these materials is exposed to an increasing applied magnetic field (H), the dipoles within the material become more likely to be aligned with the field and the magnetization (M) of the material increases. M will continue to increase until all the dipoles within the material have completely aligned with H. Saturation is reached when M is maximized and the magnetization of the material at that point is termed the saturation magnetization (M_S). Once M_S has been reached within the material, M will not continue to increase with increasing H.

In ferromagnetic material, the magnetic dipoles actually have magnetic “memory”. When ferromagnetic materials are raised above their Curie temperature (T_C = 770°C for iron), they act as paramagnets and the dipoles within the material become randomly aligned.[42] When a ferromagnet is cooled below T_C, the material abruptly becomes ferromagnetic but the dipoles are still moderately aligned and the material possesses no net magnetization. When a magnetic field is first applied the dipoles within the ferromagnet align with the field. As the polarity of the applied field is reversed, the net magnetization of the dipoles decreases. At H = 0, there is still a net magnetization within the ferromagnet, known as the remnant magnetization (M_R). As an increasingly negative H is applied, the M of the material decreases until it is 0. The absolute value of this H is known as the coercivity (H_C) of the material.

The areas enclosed by the hysteresis loop, as can be seen in Fig. 1, are defined by M_S, H_C and M_R. These represent the amount of energy lost to the environment when H goes from $H(MS)$ to $H(-M_S)$ and back. Theoretically, the total power lost to heat is given by the frequency times the integral of the *B–H curve* over a closed loop. Thus, when a ferromagnetic material is put into an oscillating/alternating magnetic field (AMF), energy will be released as heat. The larger the magnetic hysteresis curve of the ferromagnet, the “harder” that ferromagnet is said to be. “Hard” ferromagnets are used to create nanoparticles which will heat or particles which require a large H to switch their M from $+MS$ to $-M_S$ (as is desirable in magnetic data storage) while “soft” ferromagnets used applications like electric power girds to minimize energy loss. The difference in H_C between a soft and a hard ferromagnetic material can be as great as a factor of 10 000. The greater the coercivity, the higher the SAR of the nanoparticles.[43]

For hysteresis heating, there two practical limits are the frequency and magnitude of the AMF that can be applied to live animal subjects. Andrä *et al*.[44] performed calculations on whether it would be possible to use mNP hyperthermia, with a SAR value of 365 W/g, to treat small breast carcinomas while sparing the surrounding normal tissue. The estimates are also applicable to other regions of the body where blood perfusion is low. Their computational models demonstrated agreement with their experimental data, in terms of the effects of an applied magnetic field of 82 Oe (6.56 kA/m) at 400 kHz on extended cow muscle tissue. They found that for tissues with low blood perfusion, in order to avoid significant heat dose to surrounding tissue, hyperthermia should be administered as rapidly as possible and with accurate dose control.

6.4. Superparamagnetic particles

There have been a number of studies where (~2– 20 nm) superparamagnetic — typically Fe_2O_3 — nanoparticles have been used to demonstrate magnetic hyperthermia either *in vitro* or *in vivo*.[45] In several instances where the AMF was applied with and without the presence of nanoparticles, experimental controls have been lacking. Therefore, it has not always been clear whether the temperature rise observed in the tissue was resulted from the presence of the nanoparticles or through eddy current heating. The *B–H* curve for superparamagnetic particles displays no magnetic hysteresis (Fig. 1), thus it seems unlikely that significant hysteresis heating occurs when using superparamagnetic nanoparticles.

Using appropriate controls, a commercial ferrofluid consisting of 3–15nm Fe_2O_3 superparamagnetic nanoparticles and AMF exposure, Chan and Chou[10] found SAR values ranging from 60–370 mW per mg of Fe, at a frequency of 1.1 MHz and an applied field of 86 Oe (6.8 kA/m). For the highest-SAR nanoparticles, they found that, at 1 MHz and an output power density of 1MW/m^3, a temperature rise of 5°C/min could be obtained with a concentration of nanoparticles of 1 mg Fe per cm^3 of body tissue. They concluded, based on several different experiments, that Néel relaxation (rotation of the magnetization vector in the particle) was the dominant mechanism of heat generation. This type of heating occurred because it is more energetically favorable for magnetic dipoles to be aligned with crystal planes in a material than to be aligned otherwise. Thus, in an alternating magnetic field when the dipoles are rapidly realigning with the applied magnetic field, there can be "magnetic friction" of the dipoles aligning against the crystal planes which generates heat.

Hilger *et al*. completed an *in vivo* study using breast adenocaricinoma cells implanted into immunodeficient mice. They injected superparamagnetic nanoparticles (referred to as "ferrofluid") into the tumors and applied 6.5 kA/m magnetic fields at a frequency of 400 kHz and demonstrated temperature increases up to 73°C in regions within the tumors. This temperature increased resulted in significant tumor necrosis.[47]

Maier-Hauff *et al*. successfully demonstrated the tolerability of superparamagnetic iron oxide nanoparticle hyperthermia in human brain tumors. They accrued fourteen patients with glioblastoma muliforme (GBM), which is an extremely aggressive form of brain cancer. These patients received multiple treatments consisting of aminosilane-coated superparamagnetic nanoparticles injected directly into the tumor. The nanoparticles were heated by an externally applied AMF. The maximum temperature within each tumor during each treatment was between 42.4 and 49.5°C. During the course of the hyperthermia treatment, the patients also received fractionated radiation therapy. No significant toxicities were observed.[48]

Very recently, DeNardo *et al*.[15] demonstrated decreased tumor growth rates after applying AMFs to nude mice injected with antibody tagged, dextran- and PEG-coated, 20 nm diameter, superparamagnetic, iron oxide particles. It is worth noting that the applied fields

used were quite large at 700,1000 or 1300 Oe (56, 80, 104kA/m). The study also demonstrated that the nanoparticles had no observable toxicity.

6.5. Domain walls

In bulk ferromagnetic materials, magnetic dipoles do not just aligned with one another. Over great enough distances (typically less than 100 nm), there exist independent magnetic domains. Within each domain the dipoles of adjacent atoms are oriented in the same direction but the magnetization of each domain is randomly aligned with respect to its neighbor domains. When a ferromagnet is heated above its T_C and then cooled, magnetic domains form within the material in orientations such that the net magnetization of the material is zero while each domain still maintains its own net magnetization.

When a H is applied to a ferromagnet with no net magnetization, dipoles do not randomly align with the H throughout the material. In reality, domain walls move with respect to one another and change in size.[49] The domain whose magnetization is parallel to H steadily grows in size until, at M_S, this is the only remaining domain within the material.[42] As the magnitude of H decreases, the other domains within the material will increase in size until there is no net M within the material at $-H_C$.

6.6. Single-domain ferromagnetic particles

Single-domain particles are typically 20–100 nm in size, depending on the material and particle shape. In these particles, the magnetic moments either rotate together, or in a complicated manner in which domain wall motion is not involved. The classification of a single-domain particle into superparamagnetic or ferromagnetic category has almost no meaning, because at low frequencies, a particle may behave superparamagnetically, while at higher frequencies it behaves ferromagnetically. The maximum possible size for a particle to contain a single-domain depends (for a particular material) on the ratio of major to minor axis for a lenticular particle, with the smallest size corresponding to equiaxed particles. Butler and Banerjee[50] estimated the maximum possible particle size for a cube-shaped particle of $Fe_3\ O_4$ is 80 nm.

Table 1 shows some of the work completed in biological systems evaluating the efficacy of nanoparticle hyperthermia created with superparamagnetic and single-domain ferromagnetic nanoparticles.

6.7. Multi-domain ferromagnetic particles

Bulk materials or particles larger than the single-domain limit contain multiple domains. In this case, reversal of magnetization occurs by flipping of the magnetic moments in domains where the magnetic moment vector is antiparallel to the applied field. It also occurs by domain growth in other domains, which occurs at lower fields. If the applied AMF can fully saturate the magnetization, then the energy losses in multi-domain materials depend on the coercivity. The latter decreases as the reciprocal of the domain size, which, in bulk materials, is related to the grain size. Thus, for fully saturated magnetic materials, the power loss decreases with increasing domain size. As a result, multi-domain particles should be avoided if the power loss is to be maximized. Jordan *et al*. demonstrated experimentally that the power loss in single-domain ferrite particles was significantly greater than that in multi-domain nanoparticles, at all applied fields they examined (up to ~165 Oe (13.2 kA/m)).[20] The relationship between nanoparticle size, number of domains and SAR is shown in Fig. 2.

Andrä[45] compiled data from several studies and compared the efficacy of different particles. He noted that the SAR value appeared to increase linearly with increasing frequency over

the frequency range studied. The best heating occurred for iron oxide particles — mainly $Fe_2 O_3$ — with sizes in the range 20–100 nm.[45]

Rand *et al*.[51,52] injected large, uncoated multi-domain ferrosilicone particles (100–1000 nm) into rabbits, and applied a low-frequency AMF of 2 kHz at a high field strength of 1000 Oe (80kA/m). The rabbit's kidneys were determined to reach 55°C in 1–2 min. After the kidneys cooled, they performed further heat treatments, raising the kidney temperature to 43°C up to three times. They found extensive cancer cell necrosis. In later treatments, they raised the temperature to 50°C, but cooled the kidneys more slowly after treatment. This latter treatment killed all kidney tumor cells. All animals survived the treatments. They found that rabbits exposed to these magnetic fields for up to 30 min did not show ill effects even after three years with the presence of the nanoparticles in the lungs and kidneys.

Since this preliminary work has been completed, there have been few additional studies using multi-domain ferromagnetic nanoparticles *in vivo* for cancer therapy. This is due to a shift toward using superparamagnetic and single-domain ferromagnetic nanoparticles.

7. Challenges of mNPH

Recently, Keblinski *et al*.[53] used a diffusive heat equation to show that, because of the large thermal diffusivity in cells, which are essentially water, it is impossible for either a single-particle or many particles to produce significant localized heating. A large concentration of particles, however, are capable of producing significant global heating in a tissue. The results of these calculations are similar to those done by Rabin.[54]

An extension of the work by Keblinski and Rabin is the implication that the SAR of the nanoparticles determines the minimum size of treatable tumor. Hergt *et al*.[55] showed that if a tumor contains no more than 0.1 mg/mm^3 of nanoparticles, with SAR values of 50, 500 and 5000 W/g, the minimum size of tumor that can be heated to a temperature sufficient for hyperthermia treatment is 2, 0.6 and 0.1 mm. It is worth noting that 5000 W/g may be unachievable due to biological constraints on AMF strength and frequency and the properties of materials used to make nanoparticles.

Clustering of nanoparticles is commonly observed in tumors.[56] Figure 3 shows the clustering of nanoparticles within a mouse tumor. This clustering has been shown to affect the SAR in gel–nanoparticle systems.[19,57] Thus, there is significant evidence that the arrangement of nanoparticles in cellular structures is critical to their role in AMF heating. Little has been done, however, to fully understand or exploit this behavior. Abraham *et al*.[58] have shown that magnetic fields on the order of 0.3–3 T (comparable to those experienced in MRI coils) are sufficient to drive the formation of chains of nanoparticles, and other linked structures.

8. Non-Iron Oxide Magnetic Nanoparticles

As noted, one of the most important characteristics of magnetic nanoparticles for anti-cancer hyperthermia is high SAR. High nanoparticle SAR allows for high CEM43°C in the tumor while minimizing the eddy current and diamagnetic heating in normal tissue. Iron-core, iron oxide-shell nanoparticles have been successfully developed to improving the SAR of iron oxide nanoparticles while simultaneously improve the utility of therapeutic nanoparticles as MRI contrast agents.[59] The ability to visualize the biodistribution of nanoparticles before heating them is projected to aid in treatment planning.

Nanoparticles with a Fe core and passivating epitaxial shell of MgO have been synthesized via chemical vapor condensation[60] for hyperthermia applications. Nanoparticles produced

by Chatterjee *et al*. are encapsulated in polyethylene glycol and can include drugs which are released upon thermal activation.[61] Cobalt[62] and iron–cobalt alloys[63,64] have attractive SAR values but may have toxic properties.[41]

Another novel form of mNP have self-limited heating properties (tunable T_C). Their maximum temperature is typically set to that required for cytoxicity in tumors.[65–68] Unfortunately, as with the nanoparticles containing Co, Cu and Ni, this requires the use of elements such as Sr, La, Y, Mn, Ag or Al, whose toxicity effects as nanoparticles are unknown.

9. Nanoparticle Selection

There does not appear to be an ideal particle for all magnetic heating applications. Iron oxide particles, often coated with dextran, are the most commonly used because they have excellent biocompatibility with almost no toxicity[15,69] and very high SAR/heating values.[10]

The optimum particle for heating depends on the AMF frequency and field strength, and nanoparticle size (ability to enter tumor) and shape. Hergt *et al*.[70] illustrated the importance of these points by examining the power loss per unit weight for three different average sizes of Fe_3O_4 particles, some of which were equi-axed, and some of which were lenticular (from 250–1500nm). Each showed different hysteresis loops. They found a crossover in power loss behavior, where the particles that showed the largest power loss at low applied fields exhibited the least loss at high fields.

For power loss due to Néel relaxation, the optimum particle size decreased with increasing frequency.[70] A key feature of Néel relaxation power loss of a superparamagnetic nanoparticle is that sizes below the optimum lose power at significantly lower rates than particles that are the optimum size, indicating that a monodispersed particle size is the ultimate goal. Hergt *et al*.[70] showed that the power loss per unit weight for ferrofluid (single-domain) Fe_3O_4 nanoparticles increased with increasing particle size at 300 kHz and 82 Oe (6.56 kA/m). Later, Hergt *et al*.[55] showed that by changing the particle size distribution in a batch of ferrofluidic Fe_3O_4 nanoparticles with average initial particle size of 13 nm, such that the average particle size increased, while the distribution width decreased, the power loss at 410 kHz increased dramatically.

10. Synthesis of Magnetic Nanoparticles

10.1. Standard precipitation

The conventional method of producing magnetite nanoparticles utilizes the coprecipitation of a 2:1 mixture of Fe^{3+} and Fe^{2+}, in a nonoxidizing alkaline (pH = 8–14) environment. The overall reaction is:

$$Fe^{2+} + Fe^{3+} + 8OH^- \rightarrow Fe_3O_4 + 4H_2O. \quad (4)$$

An-oxygen-free environment is required to prevent the following reaction from producing Iron (III) hydroxide:

$$Fe_3O_4 + 0.25O_2 + 4.5H_2O \rightarrow 3Fe(OH)_2. \quad (5)$$

When carried out in bulk solution, the reaction kinetics must be carefully tailored to control the particle size distribution. Such control is obtained by separating the process into nucleation and growth steps. Supersaturating the salt solution ensures that nucleation occurs

simultaneously. Ideally, after nucleation, only growth takes place, resulting in a narrow size distribution. A wide variety of reaction conditions can be varied to tailor the size, magnetic properties, and surface properties.[69]

10.2. Nanoreactors

To more easily control the size distribution during synthesis, various techniques have been employed to physically confine synthesis reactions. An archetypical example is the water in oil emulsion system which typically consists of water, reagents, a surfactant, a co-surfactant, and oil. In this case, iron salt reagents are present in a stable aqueous dispersion within an oil phase. Dispersion of water in the oil phase is made possible by surfactants and co-surfactants, which lower the water/oil interfacial tension. Varying system temperature along with the amount of surfactant/co-surfactant allows control over the size of the nanoreactor. Phospholipids can naturally form vesicles around magnetite particles[71] and are used in an analogous fashion to water in oil emulsion confinement.[72] Synthesis and stabilization of mNPs has been accomplished inside dendrimers,[73] and cyclodextrins.[74] Ferittin, a protein that stores iron in “cage” like fashion, is used as a nanoreactor as well.[75–77] Size distributions having standard deviations on the order of 1 nm have been achieved using ferritin proteins; and, through genetic modification, cancer-specific targeting peptides can be incorporated into ferrittin cages giving this technology innate targeting capabilities.[78]

10.3. Sol-gel

Additional wet chemical methods include sol–gel and polyol methods. In these methods, molecular iron oxide precursors (i.e., iron salts) are “polymerized” into nanoparticulate structures through OH group linkages in a solvent at room temperature; this creates the sol-phase of the process. Upon completion of the precursor sol-phase further heat treatments are applied to generate the final chemical and structural state.[69] For example, silica-encapsulated γ-Fe_2O_3 particles in the 6–15 nm range have been produced by 400°C heat treatment of $Fe(NO_3)_3 9H_2O$ sols in tetraethylorthosilicate.[79] By varying the solvents, salts, reagent concentrations, reaction temperature, pH, and agitation, particle size, composition and microstructure can be controlled. This method has the advantage of allowing the formation nano-composite structures,[69] such as Fe_2O_3–SiO_2.[80] In a related process, polyols (polyaclohols) are used to solubilize metal-oxide precursor molecules. The polyol is then boiled, during which the metal precursors reduce and nucleate to form particles. Polyols are advantageous due to the higher reaction temperature allowing for better crystallinity and *in situ* coating of hydrophilic polyol groups which permits aqueous dispersion of the particles.[69] Nanoparticles were successfully produced in this manner using triethylene glycol.[81]

Hydrothermal synthesis routes usually involve either hydrolysis or oxidation of iron salts or neutralization of mixed metal hydroxides.[69,82] Solvent type, reaction temperature, and presence of a surfactant are primarily used to control particle size by influencing the kinetics of growth and nucleation. For example, higher temperatures may favor nucleation over growth of existing nuclei, resulting in smaller particle size.[83] Other high temperature synthesis routes include thermal decomposition of iron precursors, such as iron pentacarbonyl. Park *et al*. produced monodispersed magnetite particle solutions with sizes ranging from 4 to 11 nm, depending on reaction temperature.[84]

Additional high temperature synthesis routes employing aerosol and vapor methods have been found. Maghemetite particles from 5 to 60 nm have been produced by the spray pyrolosis method. Iron precursors, typically in an organic solvent, are aerosolized and sprayed into reactors where the precursor nucleates as the solvent evaporates; particle morphology is dependent on the precursor solution.[69,85] Laser pyrolysis of iron

pentacarbonyl vapors in a flowing ethylene/air gas stream has been used to produce magnetite nanoparticles with very narrow size distributions, and can be tuned by changing the ethylene/air gas composition, flow rate, or laser power.[80–89]

10.4. Stabilization

Bare magnetic nanoparticles do not form stable aqueous colloidal suspensions. Creation of a stable ferrofluid requires nanoparticles be coated with a surfactant that augments either stearic or electrostatic repulsive forces. The choice of surfactant is critical to the end-use of a given nanoparticle technology; many commonly used surfactants are not biocompatible, limiting medical applications of iron oxide nanoparticles. Generally, coatings are applied *in situ* during synthesis and thus play a role in the above synthesis. Citric acid, for example, has been used to stabilize magnetite particles produced via coprecipitation of iron salts; its concentration during synthesis has an effect on nanoparticle size.[90] The carboxyl groups on citric acid coordinate to the particle's surface adding hydrophilic and negatively charged properties.[69] It has been found, however, that excess carboxylates negatively impact the crystallinity of iron oxide nanoparticles.[91]

Inorganic materials have been used extensively to stabilize magnetic nanoparticles. Silica and other silicon-based coatings are useful because they can prevent agglomeration, improve chemical stability and be bio-inert.[92] These coatings are usually added via silanization with various organosilanes,[93–95] or from silicic acid solutions.[96] Gold is another appropriate inorganic colloidal stabilizer; by using iterative hydroxylamine seeding Au^{3+} ions have been deposited onto 9 nm magnetite nanoparticles to create hydrophilic particles 60 nm in diameter. Despite the thickness of this coating, magnetic properties of the particles remain unaffected.[97]

Some of the most widely used stabilizers of iron oxide nanoparticles are polymer-based. There are many different polymeric stabilizers; some of the most widely adopted are dextran and polyethylene glycol (PEG). Dextran, a glucan, is widely adopted for its accepted biocompatibility. Adsorption of dextran is believed to be facilitated by hydrogen bonding of hydroxyl groups to the oxide surface.[98] It is most often applied *in situ* during co-precipitation of iron salts[99] but has also been applied to particles post-synthesis.[99] PEG is another favored surfactant; it is not only biocompatible but increases a nanoparticle's blood circulation time[100] and prevents nanoparticles from being phagocytosed by the macrophages in the liver and spleen (the reticuloendothelial system).[69] It should be noted that different nanoparticles coatings can affect the magnetic properties of nanoparticles.[101–104]

Heat-labile polymer-mNP constructs are a promising development as they introduce both highly focused chemotherapeutics and highly focused heating, which would reduce systemic toxicity. The TI would also be further improved if the chemotherapeutic were one with synergistic or additive properties when used in conjunction with hyperthermia. Polymers which are both thermally responsive and biodegradable have been created which undergo transformations at physiologically acceptable temperatures and can be used to carry chemotherapeutics. An example of this is dextran-g-poly (NIPAAm-co-DMAAm) which adapts an "expanded hydrophilic structure" at temperatures below its lower critical solution temperature (LCST).[105] This LCSTcanbe "tuned" with the addition of co-monomer units. At temperatures above the LCST, the polymer adapts "compact hydrophobic structure" which exposes the chemotherapeutic conjugated to the iron oxide core.[106]

11. Enhanced Permeability and Retention (EPR) Effect

For a tumor to grow beyond approximately two millimeters in diameter, tumor cells must excrete a variety of molecular signalers to initiate blood vessel growth and recruit

nutrients.[107] The growth of new blood vessels is termed “neovascularization” or “angiogenesis”. Tumoral angiogenesis typically is disorganized, occurring rapidly. This type of vascularization results in large (600–800 nm) fenestrations (gaps) between adjacent tumor endothelial cells.[108] These fenestrations permit substances injected into the blood — for instance, gadolinium contrast used to increase signal within tumor tissues during MRI imaging — to accumulate within tumors, even without any targeting moiety present.[109] By injecting nanoparticles systemically, it is hoped that a large percentage of the injected dose will accumulate within tumors due to the EPR effect.[110]

The EPR effect is demonstrated in Fig. 4.

For an intravenously-administered molecule to be able to reach the tumor, it must avoid clearance by (predominantly) four organs: kidneys, liver, spleen and bone marrow.[111] The degree and mode of clearance is significantly dependent upon nanoparticle size and surface chemistry. The kidneys will rapidly clear most molecules less than approximately 10^4 atoms (several nanometers) in size.[111] The reticuloendothelial system (RES) is composed of immune cells — predominantly macrophages — present in the liver and spleen which remove certain macromolecules from circulation, especially when they are hydrophobic, charged[112,113] and large (approximately 100–300nm hydrodynamic diameter).[114]

Nanoparticle size and surface characteristics will affect their tumor localization and overall biodistribution *in vivo*. As noted, nanoparticles over 100 nm in diameter and particles with more hydrophobic coatings will be rapidly depleted from circulation through RES filtration.[100] Smaller particles are therefore more desirable from a distribution standpoint as well as for penetration and diffusion by the EPR effect. Nanoparticles of decreasing size, however, have higher surface area to volume ratios which favors plasma protein adherence. With significant protein agglomeration, the particles will again be recognized and cleared by reticuloendothelial macrophages.[115] Since surface coatings, along with targeting moiety attachment, to the nanoparticle will determine the final hydrodynamic diameter, the ability to decrease surface thickness while ensuring stability and maintaining sizeable crystal cores is invaluable.

12. Nanoparticle Targeting

Specific epitopes and receptors associated with cancer cells may be targeted using functional groups. Due to their mutated genotype, tumor cells often produce unique or overexpressed markers (antigens) which distinguish them from normal cells. These markers may then be exploited for targeting purposes. For example, the breast cancer marker Her2 is frequently over-expressed as a surface receptor in breast tumors and is therefore of targeting interest.[116] Another strategy involves targeting tumor-associated antigens such as VEGF, which is a factor involved in angiogenesis.[117]

Various organic and inorganic polymer coatings can be chemically-modified to display functional groups, forming the basis for conjugation of other targeting ligands. Examples of synthetic polymer coatings include poly(vinyl alcohol), poly(lactic-co-glycolic acid) and PEG.[118–121]Natural polymers like dextran and chitosan are also commonly used.[119,122] Although some of these polymers are intrinsically cationic or anionic, they may all be modified with the addition of terminal groups such as amines, carboxylic acids and thiols to influence surface charge.

Upon the application of functionalized coatings, nanoparticles may have a variety targeting moieties added (demonstrated in Fig. 5), depending on the intended cancer target or associated function. Folic acid is one of the most frequently conjugated ligands, as it preferentially targets cancer cells and folate receptor binding results in particle

endocytosis.[123,124] Other common targeting ligands include therapeutically relevant peptides and derivations of antibodies. Proven anti-cancer antibodies such as Herceptin (anti-Her2) have been conjugated in full IgG form successfully to nanoparticles. The decreased size and increased availability of engineered Fab (fragment, antigen binding) or scFv (single-chain variable fragment) fragments of these antibodies, however, can provide more flexibility in determining the final hydrodynamic diameter as well as available coupling chemistries.[125] The number of ligands which can be conjugated to a given nanoparticle depends on available particle surface binding sites, particle surface area and the stearics of the ligand. The latter condition may be mediated by using linker molecules (such as bi-functionalized PEG) as spacers between the ligand and the particle surface, but at the expense of increased size.

13. Conclusion: Requirements for Magnetic Nanoparticles Used in Cancer Therapy

Producing localized hyperthermia of malignant lesions, using nanoparticles and AMF, has the potential to either directly kill the cancer cells or enhance susceptibility to radiation or chemotherapy. Several critical developments are needed to make nanoparticle-based hyperthermia clinically viable:

- **i.** The nanoparticles need to be coated for bio-compatibility, low toxicity and evasion of the RES and kidney filtration.
- **ii.** Nanoparticles in tumors must be selectively heated via focused AMF, leaving nanoparticles that collect in potentially vulnerable regions (liver, kidney) unheated.
- **iii.** Nanoparticles must absorb enough power to achieve cytolytic tumor temperatures (CEM43°C of greater than 60), without significant heating of the surrounding tissue.
- **iv.** It is desirable that the nanoparticles be observable *in vivo* noninvasively — such as with MRI or fluorescence imaging — to ensure that they are localized in the tumor.
- **v.** The temperature rise in the tumor must be monitored in real time during the hyperthermia treatment to allow for high TI and to compensate for changes blood flow and physiological response to heating.
- **vi.** The treatment effectiveness needs to be accurately assessed so that the issues such as nanoparticle dose and administration technique, temperature, treatment time and the number of treatments effect can be optimized.
- **vii.** For treatment of nonlocalized tumors (metastases), the nanoparticles must be targeted to improve selectivity of nanoparticles to tumors and supporting tissues.
- **viii.** Although there is potential for use of mNPH as a nontargeted monotherapy, the greatest potential for mNPH is likely due to its ability to act as an adjuvant or targeted therapy; these possibilities must be further explored.

Acknowledgments

The authors gratefully acknowledge the support of the Norris Cotton Cancer Center (Dartmouth Hitchcock Medical Center), NCI support grant: P30 CA023108-32.

References

1. Tallman MS, et al. N. Engl. J. Med. 1997; 337:1021. [PubMed: 9321529]
2. Pui CH, Robison LL, Look AT. Lancet. 2008; 371:1030. [PubMed: 18358930]

3. Jemal, A., et al. A Cancer J. Clin. Vol. 58. CA: 2008. p. 71
4. Roizin-Towle L, Pirro JP. Int. J. Radiat. Oncol. Biol. Phys. 1991; 20:751. [PubMed: 2004951]
5. McWhinney SR, Goldberg RM, McLeo HL. Mol. Cancer Ther. 2009; 8:10. [PubMed: 19139108]
6. Marchini S, D'Incalci M, Broggini M. Curr. Med. Chem. Anti-Cancer Agents. 2004; 4:247.
7. Hoeijmakers JHJ. Nature. 2001; 411:366. [PubMed: 11357144]
8. Rosen EM, Fan S, Rockwell S, Goldberg ID. Cancer Invest. 1999; 17:56. [PubMed: 10999050]
9. Gilchrist RK, et al. Ann. Surg. 1957; 146:596. [PubMed: 13470751]
10. Chan KW, Chou CK. Int. J. Hyperthermia. 1993; 9:831. [PubMed: 8106824]
11. Wust P, et al. Lancet Oncol. 2002; 3:487. [PubMed: 12147435]
12. Jordan A, et al. Int. J. Hyperthermia. 1993; 9:51. [PubMed: 8433026]
13. Moghimi SM, Hunter AC, Murray JC. Pharmacol. Rev. 2001; 53:283. [PubMed: 11356986]
14. Ito A, et al. Cancer Lett. 2004; 212:167. [PubMed: 15279897]
15. DeNardo SJ, et al. Clin. Cancer Res. 2005; 11:7087s. [PubMed: 16203807]
16. DeNardo SJ, et al. J. Nucl. Med. 2007; 48:437. [PubMed: 17332622]
17. Wieder ME, et al. Photochem. Photobiol. Sci. 2006; 5:727. [PubMed: 16886087]
18. O'Neill BE, Li KCP. Int. J. Hyperthermia. 2008; 24:506. [PubMed: 18608574]
19. Dennis CL, et al. Nanotechnology. 2009; 20:395103. [PubMed: 19726837]
20. Jordan, A., et al. Magnetic fluid hyperthermia. In: Häfeli, U.; Schütt, W.; Teller, J.; Zborowski, M., editors. Scientific and Clinical Applications of Magnetic Carriers. New York: Plenum Press; 1997. p. 569-595.
21. Ito A, Matsuoka F, Honda H, Kobayashi T. Cancer Gene Therapy. 2003; 10:918. [PubMed: 14712318]
22. Oleson JR, et al. Amer. J. Clin. Oncology. 1988; 11:368.
23. Horsman MR, Overgaard J. Clin. Oncol. 2007; 19:418.
24. Ryu KS, et al. Gynecol Oncol. 2004; 94:325. [PubMed: 15297169]
25. Needham D, Dewhirst MW. Adv. Drug Deliv. Rev. 2001; 53:285. [PubMed: 11744173]
26. Petryk AA, Giustini AJ, Ryan P, Strawbridge RA, Hoopes PJ. Energy-Based Treatment of Tissue and Assessment V. 2009; 7181:71810N.
27. Jain TK, et al. Mol. Pharm. 2005; 2:194. [PubMed: 15934780]
28. Zhang J, Misra RDK. Acta Biomater. 2007; 3:838. [PubMed: 17638599]
29. Takemoto M, et al. Int. J. Hyperthermia. 2003; 19:193. [PubMed: 12623641]
30. Ausmus PL, Wilke AV, Frazier DL. Cancer Res. 1992; 52:4965. [PubMed: 1516052]
31. Kim M, et al. IEEE Trans. Magnetics. 2006; 42:979.
32. Sekhar KR, et al. Cancer Res. 2007; 67:695. [PubMed: 17234780]
33. Kampinga HH, Dikomey E. Int. J. Rad. Biol. 2001; 77:399. [PubMed: 11304434]
34. Cassim SM, Giustini AJ, Petryk AA, Strawbridge RA, Hoopes PJ. Energy-Based Treatment of Tissue and Assessment V. 2009; 7181:71810O.
35. Pankhurst QA, Connolly J, Jones SK, Dobson J. J. Appl. Phys. D. 2003; 36:R167.
36. Sapareto SA, Dewey WC. Int. J. Radiat. Oncol. Biol. Phys. 1984; 10:787. [PubMed: 6547421]
37. Oudkerk M, et al. Radiology. 1997; 203:449. [PubMed: 9114103]
38. Ivkov R, et al. Clin. Cancer. Res. 2005; 11:7093s. [PubMed: 16203808]
39. Kim D-H, et al. Nat. Mater. 2009; 9:1.
40. Mornet S, et al. Prog. Solid State Chem. 2006; 34:237.
41. Hergt R, Dutz S, Muller R, Zeisberger M. J. Phys.: Condens. Matter. 2006; 18:S2919.
42. Griffiths, DJ. Introduction to Electrodynamics. 3rd edn.. Upper Saddle River, NJ: Prentice-Hall; 1999. p. 280-281.
43. Baker I, Zeng Q, Li W, Sullivan CR. J. Appl. Phys. 2006; 99:08H106.
44. Andrä W, d'Ambly CG, Hergt R, Hilger I, Kaiser WA. J. Magn. Magn. Mater. 1999; 194:197.
45. Andrä, W. Magnetic Hyperthermia. In: Andrä, W.; Nowak, H., editors. Magnetism in Medicine. Berlin: Wiley-VCH; 1998. p. 455-470.

46. Gazeau F, Lévy M, Wilhelm C. Nanomedicine. 2008; 3:831. [PubMed: 19025457]
47. Hilger I, et al. Investigative Radiol. 2002; 37:580.
48. Maier-Hauff K, et al. J. Neurooncol. 2007; 81:53. [PubMed: 16773216]
49. Fischer, T. Materials Science for Engineering Students. Elsevier; Burlington, MA: 2009. p. 414-415.
50. Butler RF, Banerjee SK. J. Geophys. Res. 1975; 80:4049.
51. Rand RW, Snow HD, Elliott DG, Snyder M. Appl. Biochem. Biotech. 1981; 6:265.
52. Rand RW, Snow HD, Brown WJ. J. Surg. Res. 1982; 33:177. [PubMed: 7109564]
53. Keblinski P, Cahill DG, Bodapati A, Sullivan CR, Taton TA. J. Appl. Phys. 2006; 100:54305–54311.
54. Rabin Y. Int. J. Hyperthermia. 2002; 18:194. [PubMed: 12028637]
55. Hergt R, et al. J. Magn. Magn. Mater. 2004a; 280:358.
56. Giustini AJ, Ivkov R, Hoopes PJ. Energy-Based Treatment of Tissue and Assessment. 2009; V7181:71810M.
57. Eggeman AS, Majetich SA, Farrell D, Pankhurst QA. IEEE Trans. Magnetics. 2007; 43:2451.
58. Abraham VS, Nair SS, Rajesh S, Sajeev US, Anantharaman MR. Bull. Mater. Sci. 2004; 27:155.
59. Zhang G, Liao Y, Baker I. Mater. Sci. Eng. C. 2010; 30:92.
60. Martinez-Boubeta C, et al. Nanomedicine: NBM. 2010; 6:362.
61. Chatterjee J, Bettge M, Haik Y, Chen CJ. J. Magn. Magn. Mater. 2005; 293:303.
62. Bonnemann H, et al. Inorg. Chim. Acta. 2003; 350:617.
63. Zhang XX, Wen GH, Xiao G, Sun S. J. Magn. Magn. Mater. 2003; 261:21.
64. Hutten A, Sudfeld D, Ennen I, Reiss G, Wojczykowski K, Jutzi P. J. Magn. Magn. Mater. 2005; 293:93.
65. Kuznetsov AA, Shlyakhtin OA, Brusentsov NA, Kuznetsov OA. Eur. Cells Mater. 2002; 3:75.
66. Giri J, Ray A, Dasgupta S, Datta D, Bahadur D. Bio-Med. Mater. Eng. 2003; 13:387.
67. Melnikov OV, et al. J. Biomed. Mater. Res. Part A. 2009; 91:1048.
68. Vasseur S, et al. J. Magn. Magn. Mater. 2006; 302:315.
69. Laurent S, et al. Chem. Rev. 2008; 108:2064. [PubMed: 18543879]
70. Hergt R, et al. IEEE Trans. Magnetics. 1998; 34:3745.
71. Decuyper M, Joniau M. Langmuir. 1991; 7:647.
72. Sangregorio C, et al. J. Appl. Phys. 1999; 85:5699.
73. Strable E, et al. Chem. Mater. 2001; 13:2201.
74. Bonacchi D, et al. Chem. Mater. 2004; 16:2016.
75. Meldrum FC, et al. Science. 1992; 257:522. [PubMed: 1636086]
76. Dickson DPE, et al. Nanostruct. Mater. 1997; 9:595.
77. Wong KK, et al. Chem. Mater. 1998; 10:279.
78. Uchida M, et al. J. Amer. Chem. Soc. 2006; 128:16626. [PubMed: 17177411]
79. del Monte F, et al. Langmuir. 1997; 13:3627.
80. Solinas S, Piccaluga G, Morales MP, Serna CJ. Acta Mater. 2001; 49:2805.
81. Cai W, Wan JQ. J. Coll. Interf. Sci. 2007; 305:366.
82. Willard, MA.; Kurihara, LK.; Carpenter, EE.; Calvin, S.; Harris, VG. Encyclopedia of Nanoscience and Nanotechnology. Nalwa, HS., editor. CA: American Scientific Publishers Valencia; 2004. p. 815
83. Chen D, Xu R. Mater. Res. Bull. 1998; 33:1015.
84. Park J, et al. Ange. Chem.-Int. Edn. 2005; 44:2872.
85. Gonzalez-Carreño T, et al. Mater. Lett. 1993; 18:151.
86. Veintemillas-Verdaguer S, et al. Mater. Lett. 1998; 35:227.
87. Veintemillas-Verdaguer S, et al. J. Phys. D Appl. Phys. 2004; 37:2054.
88. Morales MP, et al. J. Magn. Magn. Mater. 2003; 266:102.
89. Alexandrescu R, et al. Appl. Surf. Sci. 2005; 248:138.

90. Bee A, et al. J. Magn. Magn. Mater. 1995; 149:6.
91. Liu C, Huang PM. Soil Sci. Soc. Amer. J. 1999; 63:65.
92. Lesnikovich AI, et al. J. Magn. Magn. Mater. 1990; 85:14.
93. Mornet S, et al. J. Magn. Magn. Mater. 2005; 293:127.
94. del Campo A, et al. J. Magn. Magn. Mater. 2005; 293:33.
95. Yamaura M, et al. J. Magn. Magn. Mater. 2004; 279:210.
96. Butterworth MD, Bell SA, Armes SP, Simpson AWJ. Coll. Interf. Sci. 1996; 183:91.
97. Lyon JL, et al. Nano Lett. 2004; 4:719.
98. Bautista MC, et al. J. Magn. Magn. Mater. 2005; 293:20.
99. Molday RS, MacKenzie D. J. Immunol. Meth. 1982; 52:353.
100. Gupta AK, Gupta M. Biomaterials. 2005; 26:3995. [PubMed: 15626447]
101. Chan, DF.; Kirpotin, DB.; Bunn, PA, Jr.. Physical chemistry and *in vivo* tissue heating properties of colloidal magnetic iron oxides with increased power absorption rates, Scientific and Clinical Applications of Magnetic Carriers. Häfeli, U.; Schütt, W.; Teller, J.; Zborowski, M., editors. Plenum Press; 1997. p. 607-618.
102. Berkowitz AE, Lahut JA. AIP Conf. Proc. 1973; 10:966.
103. Berkowitz AE, Lahut JA, Jacobs IS, Levinson LM, Forester DW. Phys. Rev. Lett. 1975; 34:594.
104. Morrish, AH. Studies of magnetic properties of fine particles, *Surface Properties of Small Particles*. Dormann, JL.; Fiorani, D., editors. Rome: Elsevier; 1992. p. 181-190.
105. Zhang J, Misra RDK. Acta Biomater. 2007; 3:838. [PubMed: 17638599]
106. Yuan Q, Venkatasubramanian R, Hein S, Misra RDK. Acta Biomater. 2008; 4:1024. [PubMed: 18329348]
107. Coffelt SB, Hughes R, Lewis CE. Biophys. Acta. 2009; 1796:11.
108. Wang X, Yang L, Chen Z, Shin DM. CA: A Cancer J. Clin. 2008; 58:97.
109. Greish K. J. Drug Targeting. 2007; 15:457.
110. Sutton D, et al. Pharm. Res. 2007; 24:1029. [PubMed: 17385025]
111. Maeda H. Advances in Enzyme Regulation. 2001; 41:189. [PubMed: 11384745]
112. Shan X, et al. Coll. Surf. B Biointerf. 2009; 72:303.
113. Chouly C, Pouliquen D, Lucet I, Jeune JJ, Jallet P. J. Microencapsulation. 1996; 13:245. [PubMed: 8860681]
114. Gaumet M, Gurny R, Delie F. Eur. J. Pharm. Sci. 2009; 36:465. [PubMed: 19124077]
115. Torchilin VP, Trubetskoy VS. Adv. Drug Del. Rev. 1995; 16:141.
116. Slamon DJ. Cancer Invest. 1990; 8:253. [PubMed: 1976032]
117. Chen J, Wu H, Han D, Xie C. Cancer Lett. 2006; 231:169. [PubMed: 16399221]
118. Petri-Fink A, Chastellain M, Juillerat-Jeanneret L, Ferrari A, Hofmann H. Biomaterials. 2005; 26:2685. [PubMed: 15585272]
119. Pardoe H, Chua-anusorn W, Pierre TGSt, Dobson J. J. Magn. Magn. Mater. 2001; 225:41.
120. Lee SJ, et al. Coll. Surf. A: Physicochem. Eng. Asp. 2005; 255:19.
121. Zhang Y, Kohler N, Zhang M. Biomaterials. 2002; 23:1553. [PubMed: 11922461]
122. Chang YC, Chen DH. J. Coll. Interf. Sci. 2005; 283:446.
123. Choi H, et al. Acad. Radiol. 2004; 11:996. [PubMed: 15350580]
124. Sonvico F, et al. Bioconjugate Chem. 2005; 16:1181.
125. Holliger P, Hudson PJ. Nat. Biotech. 2005; 23:1126.
126. Jordan A, et al. J. Magn. Magn. Mater. 1999; 194:185.
127. Hilger I, et al. Radiology. 2001; 218:570. [PubMed: 11161180]
128. Ito A, et al. Cancer Sci. 2003; 94:308. [PubMed: 12824927]
129. Kikumori T, Kobayashi T, Sawaki M, Imai T. Breast Cancer Res. Treat. 2009; 113:435. [PubMed: 18311580]
130. Hoopes PJ, et al. Energy-Based Treatment of Tissue and Assessment V. 2009; 7181:71810P.

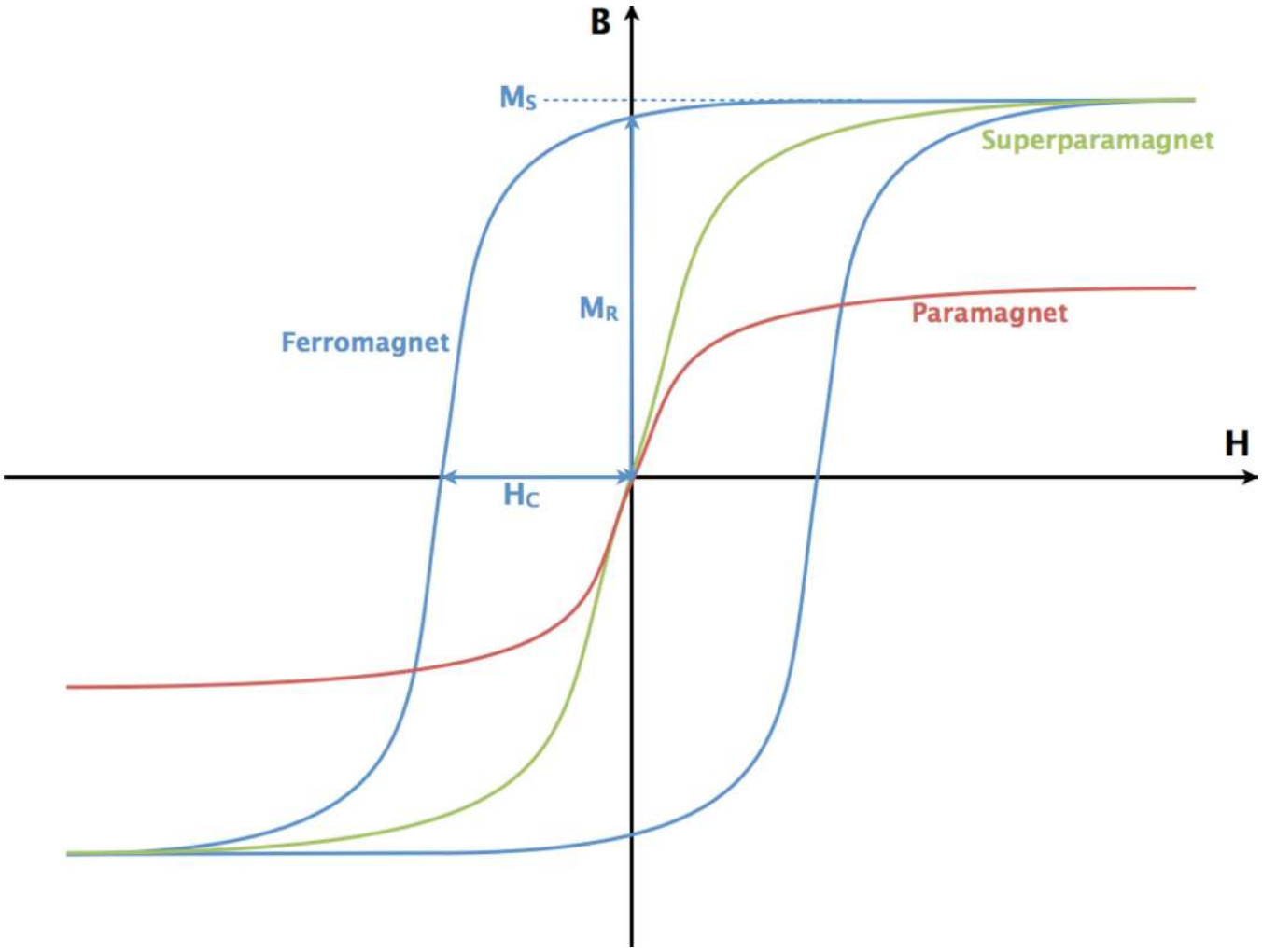

Fig. 1.

B is the total magnetic field and *H* is the applied magnetic field in a sample. The hysteresis curves of various types of bulk materials are shown here. For the ferromagnetic material (blue), the saturation magnetization (M_S), coercivity (H_C) and remnant magnetization (*Mr*) are indicated. The *B*–*H* curves of superparamagnetic (green) and paramagnetic (red) materials are also shown; these two types of materials demonstrate no magnetic hysteresis (no area enclosed by *B*–*H* the curve) (color online).

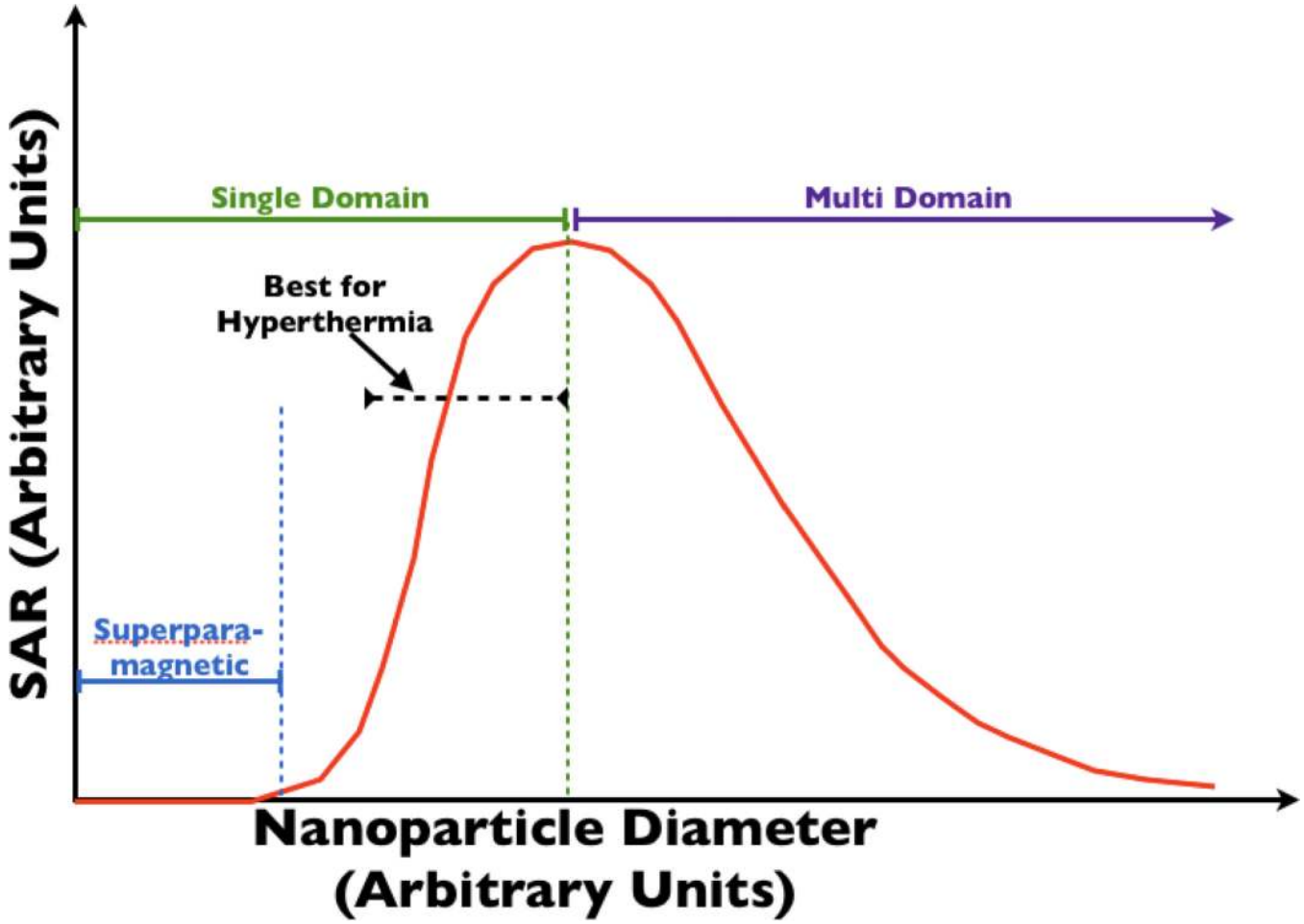

Fig. 2.
This figure shows the dependence of SAR on nanoparticle diameter. Single-domain particles, whose size is close to the single-domain/multi-domain transition size, are desirable for their high SAR and smaller size.

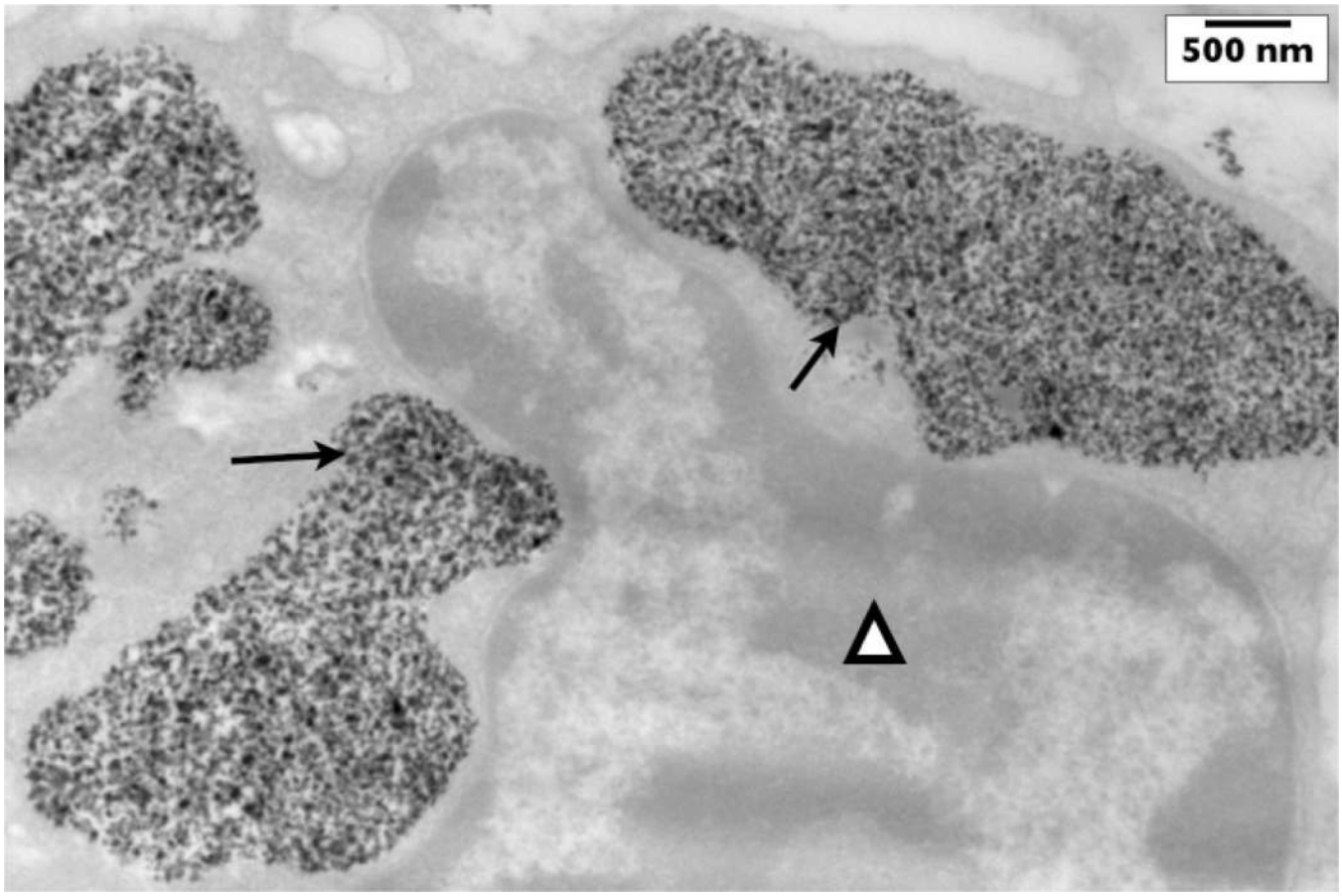

Fig. 3.
This TEM image demonstrates ferromagnetic nanoparticles inside of vesicles within a murine adenocarcinoma cell (arrows). The cell's nucleus (triangle) is shown adjacent to the nanoparticle collections. Nanoparticles were injected into this mouse tumor five hours before the tumor was excised and fixed for TEM.

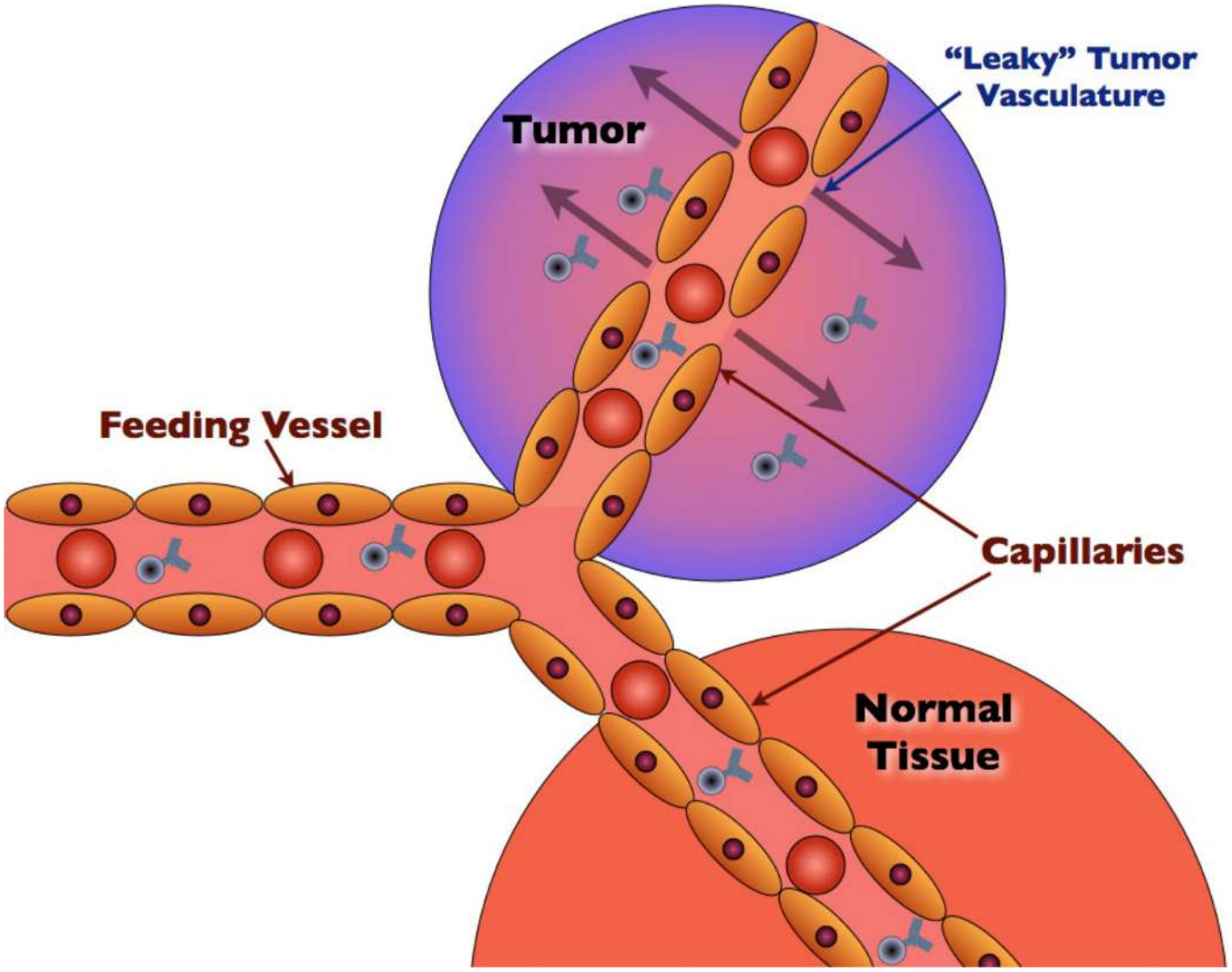

Fig. 4.
The EPR (enhanced permeability and retention) effect allows for preferential diffusion of substances present in the blood into tumors (as shown with the schematic of targeted nanoparticles in this figure).

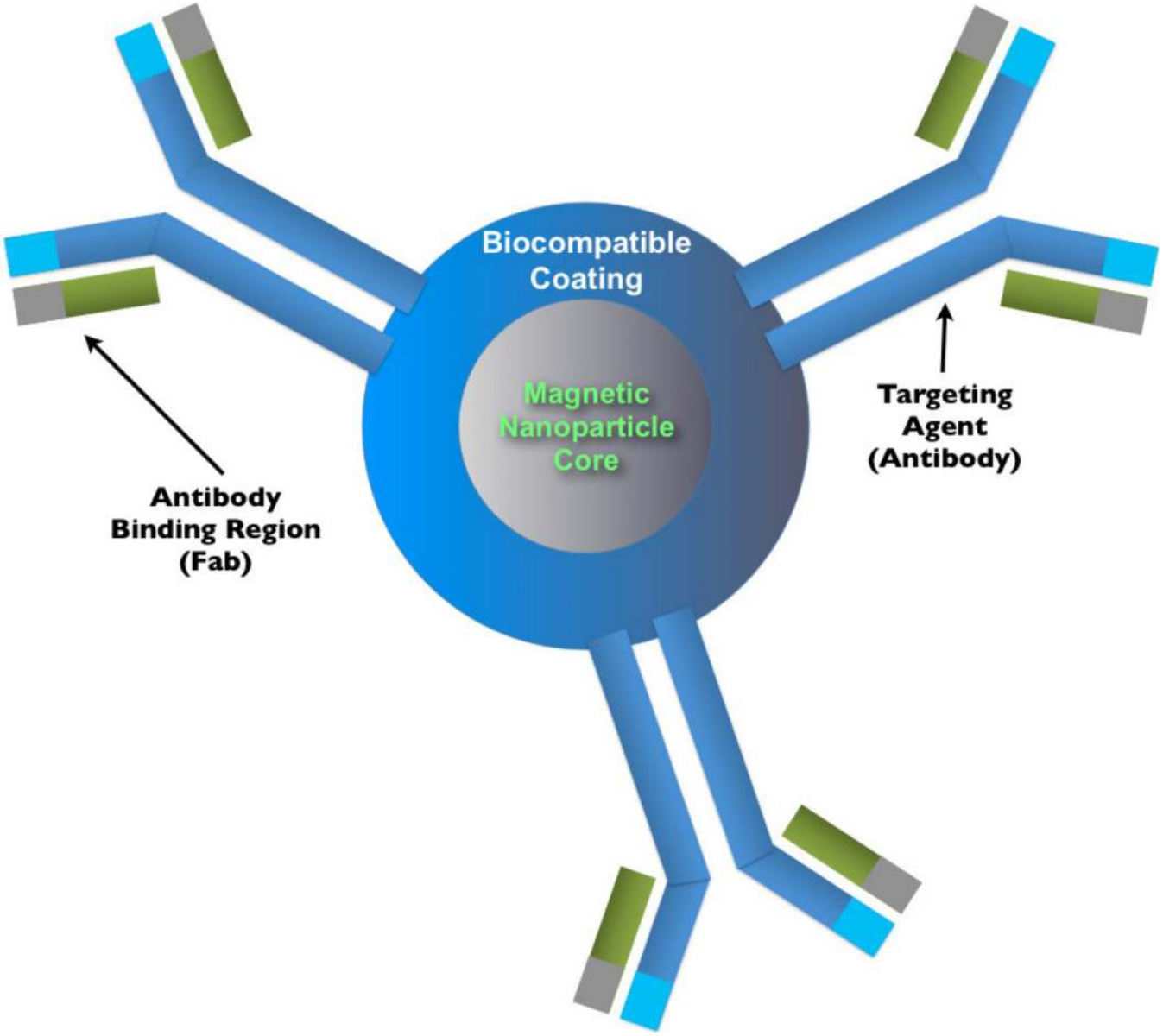

Fig. 5.
A schematic of a nanoparticle conjugated to targeting agents. In this schematic, the nanoparticle is conjugate to several antibodies.

Table 1

This table describes many of the nanoparticle hyperthermia studies which have been done in biological settings.

Group	Year	Particles used	Experimental setting	Effect seen
Jordan et al.[126]	1999	Dextran or aminosilane-coated magnetite. Superparamagnetic. 3–13 nm crystal diameters.	*In vitro*	Similar cytotoxic efficacy of water bath and mNP hyperthermia when used to heat cell cultures.
Hilger et al.[127]	2001	Magnetite nanoparticles of several different shapes, aspect ratios and hydrodynamic diameters.	Ex vivo (human breast tissue) and *in vivo* (tumors in mice)	Significant average temperature increases in both ex vivo and *in vivo* treated tissues. During experiments, there was little increase in mouse core body temperature.
Hilger et al.[47]	2002	Coated magnetite. Superparamagnetic. 10nm and 200nm hydrodynamic diameter.	*In vivo* (tumors in mice)	Heterogenous tumor heating. 12–73°C temperature increase seen within tumors.
Ito et al.[128]	2003	Magnetite nanoparticles coated with lipid membrane. Administered with Interleukin-2 (IL-2).	*In vivo* (tumors in mice)	Significant improvement in mouse survival and tumor regrowth delay.
Maier-Hauff et al.[48]	2007	Aminosilane-coated iron oxide. Superparamagnetic. 15 nm crystal diameter.	*In vivo* (human brain tumors)	Little toxicity seen in human patients after brain tumors heated to 42.4–49.5°C and treated with therapeutic radiation.
DeNardo et al.[16]	2007	Dextran- and PEG-coated iron oxide, conjugated to Chimeric L6 antibody. Superparamagnetic. 20 nm hydrodynamic diameter.	*In vivo* (tumors in mice)	Significant tumor growth delay.
Kikumori et al.[129]	2009	Iron-based magnetic nanoparticles (10nm crystals) loaded into liposomes. Liposomes conjugated to Trastuzumab antibody.	*In vivo* (tumors in mice)	Significant tumor necrosis and growth delay with some complete responses.
Dennis et al.[19]	2009	Ferromagnetic, dextran-coated nanoparticles. Average hydrodynamic diameter of approximately 100 nm.	*In vivo* (tumors in mice)	Significant tumor regrowth delay.
Hoopes et al.[130]	2009	Ferromagnetic, dextran-coated nanoparticles. Average hydrodynamic diameter of approximately 100 nm.	*In vitro* and *in vivo* (tumors in mice)	Significant tumor regrowth delay. Additive effects seen with chemotherapy and radiation.